



Search for B_c^+ decays to the $p\bar{p}\pi^+$ final state

The LHCb Collaboration



ARTICLE INFO

Article history:

Received 23 March 2016

Received in revised form 29 April 2016

Accepted 23 May 2016

Available online 1 June 2016

Editor: L. Rolandi

ABSTRACT

A search for the decays of the B_c^+ meson to $p\bar{p}\pi^+$ is performed for the first time using a data sample corresponding to an integrated luminosity of 3.0 fb^{-1} collected by the LHCb experiment in pp collisions at centre-of-mass energies of 7 and 8 TeV. No signal is found and an upper limit, at 95% confidence level, is set, $\frac{f_c}{f_u} \times \mathcal{B}(B_c^+ \rightarrow p\bar{p}\pi^+) < 3.6 \times 10^{-8}$ in the kinematic region $m(p\bar{p}) < 2.85 \text{ GeV}/c^2$, $p_T(B) < 20 \text{ GeV}/c$ and $2.0 < y(B) < 4.5$, where \mathcal{B} is the branching fraction and f_c (f_u) is the fragmentation fraction of the b quark into a B_c^+ (B^+) meson.

© 2016 The Author(s). Published by Elsevier B.V. This is an open access article under the CC BY license (<http://creativecommons.org/licenses/by/4.0/>). Funded by SCOAP³.

1. Introduction

The decays of the B_c^+ meson have the special feature of proceeding through either of its valence quarks \bar{b} or c , or via the annihilation of the two.¹ In the Standard Model, the decays with a b -quark transition and no charm particle in the final state can proceed only via $\bar{b}c \rightarrow W^+ \rightarrow u\bar{q}$ ($q = d, s$) annihilation, with an amplitude proportional to the product of CKM matrix elements $V_{cb} V_{uq}^*$. Cabibbo suppression $|V_{us}/V_{ud}| \sim 0.2$ implies that final states without strangeness dominate. Calculations involving two-body and quasi two-body modes predict branching fractions in the range $10^{-8} - 10^{-6}$ [1–3]. Due to their rareness, the observation of these processes is an experimental challenge. On the other hand, any observation could probe other types of $\bar{b}c$ annihilations involving particles beyond the Standard Model, such as a mediating charged Higgs boson (see e.g. Refs. [4,5]).

The decays of B_c^+ mesons to three light charged hadrons provide a good way to study such processes. These include fully mesonic $h^+h^-h^+$ states or states containing a proton–antiproton pair and a light hadron, $p\bar{p}h^+$ ($h, h' = \pi, K$). In this study, the primary focus is on $B_c^+ \rightarrow p\bar{p}\pi^+$ decays in the region below the charmonium threshold, taken to be $m(p\bar{p}) < 2.85 \text{ GeV}/c^2$, where the only contribution arises from the annihilation process. The $b \rightarrow c$ transitions, leading to $B_c^+ \rightarrow [c\bar{c}] \rightarrow p\bar{p}h^+$ charmonium modes, are also considered. An analysis is performed to examine these different contributions in the $p\bar{p}\pi^+$ phase space. The $B^+ \rightarrow p\bar{p}\pi^+$ decays in the region $m(p\bar{p}) < 2.85 \text{ GeV}/c^2$ are used as a normalization mode to derive the quantity

$$R_p \equiv \frac{f_c}{f_u} \times \mathcal{B}(B_c^+ \rightarrow p\bar{p}\pi^+), \quad (1)$$

where \mathcal{B} is the branching fraction and f_c (f_u) represents the fragmentation fraction of the b quark into the B_c^+ (B^+) meson. The quantity R_p is measured in the fiducial region $p_T(B) < 20 \text{ GeV}/c$ and $2.0 < y(B) < 4.5$, where y denotes the rapidity and p_T is the component of the momentum transverse to the beam. The full Run 1 (years 2011 and 2012) data sample is exploited, representing 1.0 and 2.0 fb^{-1} of integrated luminosity at 7 and 8 TeV centre-of-mass energies in pp collisions, respectively.

2. Detector and simulation

The LHCb detector [6,7] is a single-arm forward spectrometer covering the pseudorapidity range $2 < \eta < 5$, designed for the study of particles containing b or c quarks. The detector includes a high-precision tracking system consisting of a silicon-strip vertex detector surrounding the pp interaction region, a large-area silicon-strip detector located upstream of a dipole magnet with a bending power of about 4 Tm, and three stations of silicon-strip detectors and straw drift tubes placed downstream of the magnet. The tracking system provides a measurement of momentum, p , of charged particles with a relative uncertainty that varies from 0.5% at low momentum to 1.0% at 200 GeV/c . The minimum distance of a track to a primary vertex (PV), the impact parameter (IP), is measured with a resolution of $(15 + 29/p_T) \mu\text{m}$, where p_T is in GeV/c . Different types of charged hadrons are distinguished using information from two ring-imaging Cherenkov detectors. Photons, electrons and hadrons are identified by a calorimeter system consisting of scintillating-pad and preshower detectors, an electromagnetic calorimeter and a hadronic calorimeter. Muons are identified by a system composed of alternating layers of iron and multiwire proportional chambers.

The online event selection is performed by a trigger [8], which consists of a hardware stage, based on information from the calorimeter and muon systems, followed by a software stage,

¹ Charge-conjugation is implied throughout the paper.

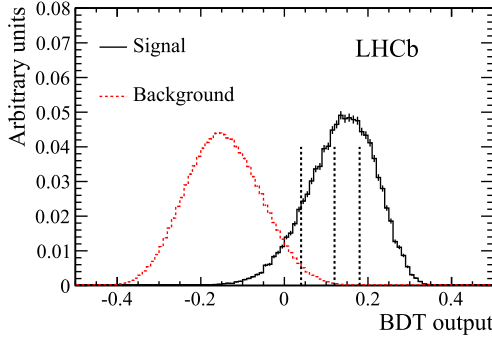


Fig. 1. Distributions of BDT output for the $B_c^+ \rightarrow p\bar{p}\pi^+$ signal and the background. The vertical dashed lines indicate the lower limits of the three regions in which the signal is determined.

which applies a full event reconstruction. At the hardware trigger stage, events are required to have a muon with high p_T or a hadron, photon or electron with high transverse energy in the calorimeters. For hadrons, the transverse energy threshold is 3.5 GeV. The software trigger requires a two-, three- or four-track secondary vertex with a significant displacement from the primary pp interaction vertices. At least one charged particle must have a transverse momentum $p_T > 1.7$ GeV/c and be inconsistent with originating from a PV. A multivariate algorithm [9] is used for the identification of secondary vertices consistent with the decay of a b hadron.

The analysis uses simulated events generated by PYTHIA 8.1 [10] and BCVEGPY [11] for the production of B^+ and B_c^+ mesons, respectively, with a specific LHCb configuration [12]. Decays of hadronic particles are described by EVTGEN [13], in which final-state radiation is generated using PHOTOS [14]. The interaction of the generated particles with the detector, and its response, are implemented using the GEANT4 toolkit [15] as described in Ref. [16].

3. Reconstruction and selection of candidates

Three charged particles are combined to form $B_{(c)}^+ \rightarrow p\bar{p}\pi^+$ decay candidates, which are associated to the closest PV. A loose preselection is performed on tracking quality, p , p_T and IP of the B_c^+ and its daughters, and B_c^+ candidate flight distance. At this stage, two windows of the invariant mass of the $p\bar{p}\pi^+$ system are retained: the B^+ region, $[5.1, 5.5]$ GeV/ c^2 , and the B_c^+ region, $[6.0, 6.5]$ GeV/ c^2 . Since the production fractions of different B species are involved, a fiducial requirement is imposed to define the kinematic region for the measurement, $p_T(B) < 20$ GeV/c and $2.0 < y(B) < 4.5$ [17].

Further discrimination between signal and background is provided by a multivariate analysis using a boosted decision tree (BDT) classifier [18]. Input quantities include kinematic and topological variables related to the B_c^+ candidates and the individual daughter particles. The momentum, vertex and flight distance of the B_c^+ candidate are exploited, as are track fit quality criteria, IP and momentum information of the final-state particles. The BDT is trained using simulated signal events, and data events from the sidebands of the $p\bar{p}\pi^+$ invariant mass $[6.0, 6.15]$ GeV/ c^2 and $[6.35, 6.5]$ GeV/ c^2 , which represent the background. To check for training biases, the signal and background samples are split into two subsamples for training and testing of the BDT output. Fig. 1 shows the distribution of the BDT output for signal and background.

Particle identification (PID) requirements are applied to reduce the combinatorial background and suppress the cross-feed of $p\bar{p}K^+$ final states in the $p\bar{p}\pi^+$ spectrum, due to the kaon being

misidentified as a pion. The BDT and PID requirements are optimized jointly in order to maximize the sensitivity to very small event yields. The B_c^+ signal yield is determined from a simultaneous fit in three bins of the BDT output X , $0.04 < X < 0.12$, $0.12 < X < 0.18$ and $X > 0.18$, each having the same expected yield (dashed lines in Fig. 1). From simulated pseudoexperiments, this method is shown to be more sensitive than a single fit to the highest signal purity region, $X > 0.18$. The normalization channel $B^+ \rightarrow p\bar{p}\pi^+$ undergoes the same PID and BDT selection, but its yield is determined without binning in BDT output.

4. Fits to the data

Signal and background yields are obtained using unbinned extended maximum likelihood fits to the distribution of the invariant mass of the $p\bar{p}\pi^+$ combinations. The $B_c^+ \rightarrow p\bar{p}\pi^+$ and $B^+ \rightarrow p\bar{p}\pi^+$ signals are both modelled by the sum of two Crystal Ball functions [19] with a common mean. For $B_c^+ \rightarrow p\bar{p}\pi^+$, all the shape parameters are fixed to the values obtained in the simulation while for $B^+ \rightarrow p\bar{p}\pi^+$, the mean and the core width are allowed to float. A Fermi function accounts for a possible partially reconstructed component from $B_c^+ \rightarrow p\bar{p}\rho^+$ ($B^+ \rightarrow p\bar{p}\rho^+$) decays, where a neutral pion from the ρ^+ is not reconstructed resulting in a $p\bar{p}\pi^+$ invariant mass below the nominal B_c^+ (B^+) mass. An asymmetric Gaussian function with power law tails is used to model a possible $p\bar{p}K^+$ cross-feed, and its contribution is found to be negligible. The combinatorial background is modelled by an exponential function. Except for this last category, all the parameters of the background components are fixed to the values obtained in simulations.

Fig. 2 shows the result of the fits in the B^+ region. For the region of interest, $m(p\bar{p}) < 2.85$ GeV/ c^2 , the yield is $N(B^+ \rightarrow p\bar{p}\pi^+) = 1644 \pm 83$, where only the statistical uncertainty is quoted. The fit to the region $2.85 < m(p\bar{p}) < 3.15$ GeV/ c^2 , which includes the $B^+ \rightarrow J/\psi(p\bar{p})\pi^+$ signal, shows the yield suppression in this region as observed in Ref. [20].

The simultaneous fits performed in the B_c^+ region are made for the region exclusive to the annihilation process, $m(p\bar{p}) < 2.85$ GeV/ c^2 , and for the charmonium region, $2.85 < m(p\bar{p}) < 3.15$ GeV/ c^2 . The fraction of the yield of the partially reconstructed background in each bin of the BDT output is constrained to be the same as in the simulation. The results are shown in Fig. 3. The corresponding signal yields are $N(B_c^+ \rightarrow p\bar{p}\pi^+) = -2.7 \pm 6.3$ for $m(p\bar{p}) < 2.85$ GeV/ c^2 and $N(B_c^+ \rightarrow p\bar{p}\pi^+) = -0.1 \pm 3.0$ for $2.85 < m(p\bar{p}) < 3.15$ GeV/ c^2 .

The main observable under consideration is determined as

$$R_p \equiv \frac{f_c}{f_u} \times \mathcal{B}(B_c^+ \rightarrow p\bar{p}\pi^+) \\ = \frac{N(B_c^+ \rightarrow p\bar{p}\pi^+)}{N(B^+ \rightarrow p\bar{p}\pi^+)} \times \frac{\epsilon_u}{\epsilon_c} \times \mathcal{B}(B^+ \rightarrow p\bar{p}\pi^+), \quad (2)$$

and a cross-check is made for the J/ψ mode

$$R_p^{J/\psi} \equiv \frac{f_c}{f_u} \times \mathcal{B}(B_c^+ \rightarrow J/\psi\pi^+) = \frac{N(B_c^+ \rightarrow J/\psi(\rightarrow p\bar{p})\pi^+)}{N(B^+ \rightarrow p\bar{p}\pi^+)} \\ \times \frac{\epsilon_u}{\epsilon_c^{J/\psi}} \times \frac{\mathcal{B}(B^+ \rightarrow p\bar{p}\pi^+)}{\mathcal{B}(J/\psi \rightarrow p\bar{p})}, \quad (3)$$

where the efficiencies ϵ are discussed in Sec. 5.

5. Efficiencies

The reconstruction and selection efficiencies are computed from acceptance maps defined in the $m^2(p\bar{p})$ vs. $m^2(p\pi)$ plane. These

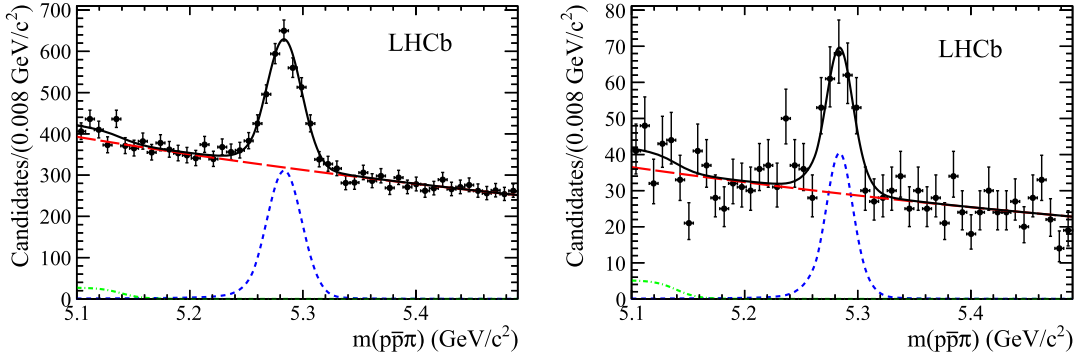


Fig. 2. Fits to the $p\bar{p}\pi^+$ invariant mass in the B^+ region, for (left) $m(p\bar{p}) < 2.85 \text{ GeV}/c^2$ and (right) $2.85 < m(p\bar{p}) < 3.15 \text{ GeV}/c^2$. The blue dashed, red long-dashed and green dotted-dashed lines represent the signal, combinatorial background and partially reconstructed background components, respectively. The error bars show 68% Poisson confidence level intervals. (For interpretation of the references to color in this figure legend, the reader is referred to the web version of this article.)

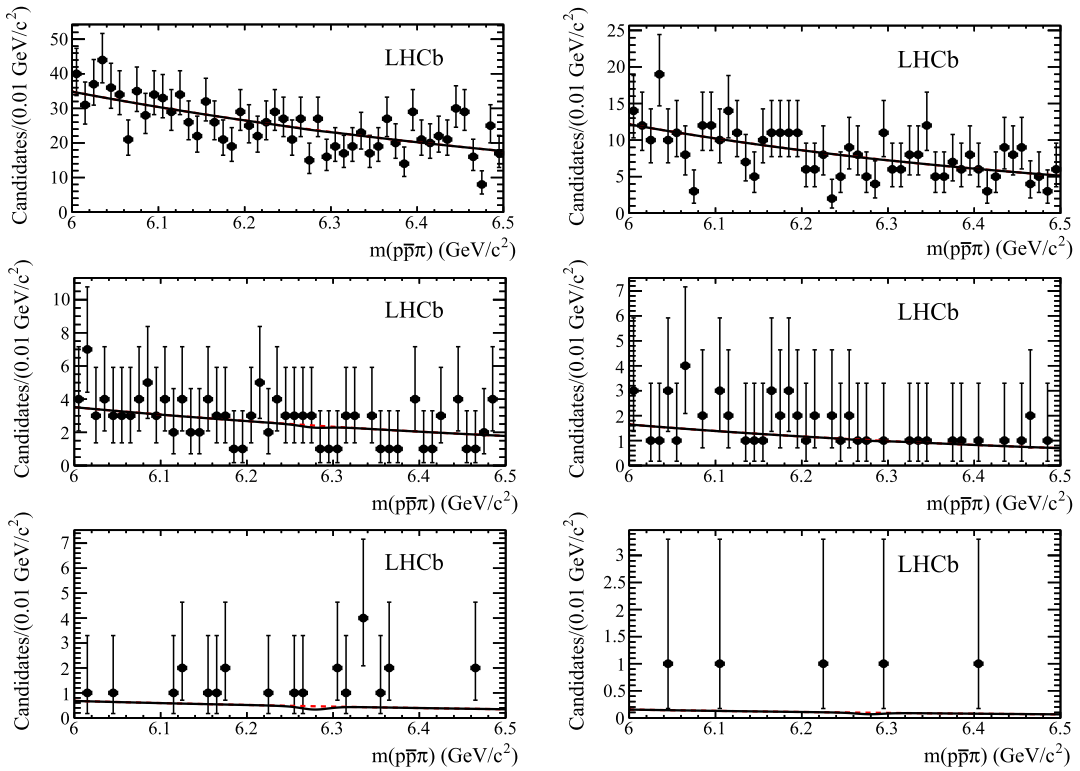


Fig. 3. Projection of fits to the $p\bar{p}\pi^+$ invariant mass in the B_c^+ region, in the bins of BDT output (top) $0.04 < X < 0.12$, (middle) $0.12 < X < 0.18$ and (bottom) $X > 0.18$, for (left) $m(p\bar{p}) < 2.85 \text{ GeV}/c^2$ and (right) $2.85 < m(p\bar{p}) < 3.15 \text{ GeV}/c^2$. The red long-dashed lines represent the combinatorial background. The signal and partially reconstructed components are too small to be shown. (For interpretation of the references to color in this figure legend, the reader is referred to the web version of this article.)

maps include the effects of event reconstruction, triggers, pre-selection, BDT and PID selections, and are obtained from simulation for both $B_c^+ \rightarrow p\bar{p}\pi^+$ and $B^+ \rightarrow p\bar{p}\pi^+$. The PID map is obtained by studying data-driven responses from calibration data samples of kinematically identified pions, kaons and protons originating from the decays $D^{*+} \rightarrow D^0(\rightarrow K^-\pi^+)\pi^+$, $\Lambda \rightarrow p\pi^-$ and $\Lambda_c^+ \rightarrow pK^-\pi^+$. The maps are smoothed using fits involving two-dimensional fourth-order polynomials. Fig. 4 shows the final combination of these maps.

To infer the average efficiency for $B^+ \rightarrow p\bar{p}\pi^+$, signal weights are calculated with the *sPlot* technique [21] from the fits shown in Fig. 2. A weight is associated with each candidate depending on its position in the $m^2(p\bar{p})$ vs. $m^2(p\pi)$ plane. The acceptance maps are then used to determine an averaged efficiency, $\epsilon_u^{\text{sel}} \equiv \langle \epsilon^{\text{sel}}(B^+ \rightarrow p\bar{p}\pi^+) \rangle$. For $B_c^+ \rightarrow p\bar{p}\pi^+$, since no signal is available in data, a simple average is performed in the region $m(p\bar{p}) < 2.85 \text{ GeV}/c^2$.

to obtain ϵ_c^{sel} , which leads to a substantial systematic uncertainty due to the variation of the efficiency over this region.

In computing the ratio $\epsilon_u^{\text{sel}}/\epsilon_c^{\text{sel}}$, three corrections are needed to account for data-simulation discrepancies: tracking efficiency, hardware hadron trigger efficiency; and the fiducial region cuts $p_T(B) < 20 \text{ GeV}/c$ and $2.0 < y(B) < 4.5$. After these corrections, $\epsilon_u^{\text{sel}}/\epsilon_c^{\text{sel}} = 2.495 \pm 0.028$ is obtained including associated systematic uncertainties.

Another efficiency ratio accounts for the fact that $B^+ \rightarrow p\bar{p}\pi^+$ and $B_c^+ \rightarrow p\bar{p}\pi^+$ decays are only detected if all the decay daughters are in the LHCb acceptance: the fractions of events satisfying this requirement are estimated by simulation and are found to be $\epsilon_u^{\text{acc}} = (18.91 \pm 0.10)\%$ and $\epsilon_c^{\text{acc}} = (15.82 \pm 0.03)\%$, which gives $\epsilon_u^{\text{acc}}/\epsilon_c^{\text{acc}} = 1.195 \pm 0.007$.

For $B_c^+ \rightarrow J/\psi(p\bar{p})\pi^+$, a similar procedure is applied and the following values are found: $\epsilon_u^{\text{sel}}/\epsilon_c^{J/\psi,\text{sel}} = 2.513 \pm 0.032$ and

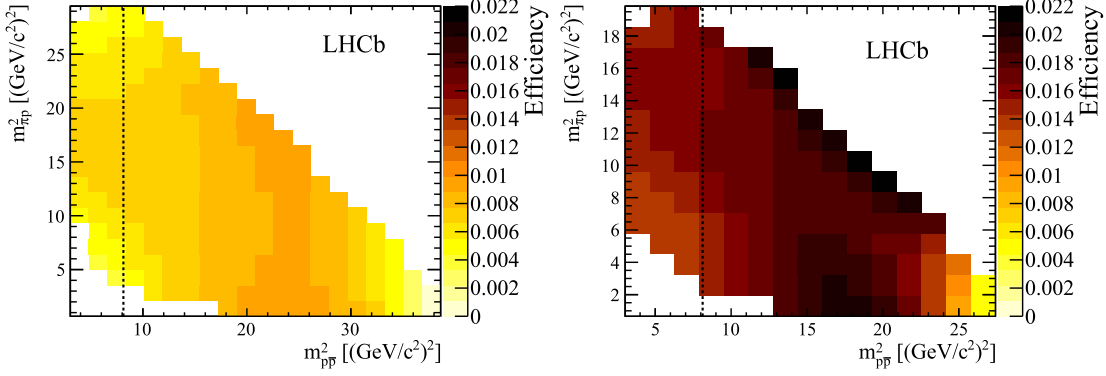


Fig. 4. Combined acceptance in the plane ($m^2(p\bar{p})$, $m^2(p\pi)$) for (left) $B_c^+ \rightarrow p\bar{p}\pi^+$ and (right) $B^+ \rightarrow p\bar{p}\pi^+$ events. The vertical dashed line corresponds to $m(p\bar{p}) = 2.85 \text{ GeV}/c^2$. (For interpretation of the colors in this figure, the reader is referred to the web version of this article.)

Table 1
Relative systematic uncertainties (in %) on the ratio ϵ_u/ϵ_c and input branching fractions.

Source	$B_c^+ \rightarrow p\bar{p}\pi^+$, $m(p\bar{p}) < 2.85 \text{ GeV}/c^2$	$B_c^+ \rightarrow J/\psi(\rightarrow p\bar{p})\pi^+$
PID	3.0	3.0
B_c^+ lifetime	2.0	2.0
Simulation	0.8	0.9
Detector acceptance	0.6	0.6
BDT shape	1.5	1.5
Hardware trigger correction	0.8	0.9
Fiducial cut	0.1	0.1
Modelling	15	—
$\mathcal{B}(B^+ \rightarrow p\bar{p}\pi^+)$	15	15
$\mathcal{B}(J/\psi \rightarrow p\bar{p})$	—	1.4

$\epsilon_u^{\text{acc}}/\epsilon_c^{J/\psi,\text{acc}} = 1.186 \pm 0.007$. The efficiency ratio used for the final results is $\epsilon_u/\epsilon_c = \epsilon_u^{\text{sel}}/\epsilon_c^{\text{sel}} \times \epsilon_u^{\text{acc}}/\epsilon_c^{\text{acc}}$. The differences between the B^+ and B_c^+ detector acceptance and selection efficiencies are caused by the different lifetimes and masses of the two mesons.

6. Systematic uncertainties

Part of the systematic uncertainties are related to the computation of the efficiency ratios, such as the PID calibration, the uncertainty in the B_c^+ lifetime, $0.507 \pm 0.009 \text{ ps}$ [22], the limited sizes of the simulation samples, the effect of the detector acceptance, the distribution of the BDT output, and the trigger and fiducial cut corrections. Others are related to the branching fractions $\mathcal{B}(B^\pm \rightarrow p\bar{p}\pi^\pm) = (1.07 \pm 0.16) \times 10^{-6}$ [20] and $\mathcal{B}(J/\psi \rightarrow p\bar{p}) = (2.120 \pm 0.029) \times 10^{-3}$ [23], or to the variation of the selection efficiency of $B_c^+ \rightarrow p\bar{p}\pi^\pm$ over the phase-space region $m(p\bar{p}) < 2.85 \text{ GeV}/c^2$, due to the lack of knowledge of the kinematics in the absence of signal in data (modelling).

Table 1 lists the different sources of systematic uncertainties. The PID uncertainty is dominated by the finite size of the proton calibration samples, which limits the sampling of the identification efficiency as a function of the track momentum and rapidity. A similar comment applies for the hardware trigger efficiency correction, where the effect is smaller due to a one-dimensional sampling as a function of the transverse momentum p_T . The uncertainty related to the differences in the BDT output shape between data and simulation has been estimated using $B^+ \rightarrow p\bar{p}h^+$ ($h = K, \pi$) samples where the signal yield has been studied as a function of the requirements on the BDT output in both data and simulation. The uncertainty on the fit model, including the knowledge of the signal shape and the contribution of the partially reconstructed background, is found to have no impact on the final result.

7. Results and summary

Upper limits on R_p and $R_p^{J/\psi}$ are estimated by making scans of these quantities, comparing profile likelihood ratios for the “signal + background” against “background”-only hypotheses [24]. From these fits, p -value profiles are inferred, the signal p -value being the ratio of the “signal+background” and “background” p -values. The point at which the p -value falls below 5% determines the 95% confidence level (CL) upper limit. In the determination of this value, the systematic uncertainties, shown in Table 1, and the statistical uncertainty on the normalization channel yield are taken into account.

The p -value scans are shown in Fig. 5, from which the following values are found: $R_p < 3.6 \times 10^{-8}$ ($m(p\bar{p}) < 2.85 \text{ GeV}/c^2$) and $R_p^{J/\psi} < 8.4 \times 10^{-6}$ at 95% CL. The latter limit is compatible with a measurement of $\frac{f_c}{f_u} \times \frac{\mathcal{B}(B_c^+ \rightarrow J/\psi\pi^+)}{\mathcal{B}(B_c^+ \rightarrow J/\psi K^+)}$ [17] from which the value $R_p^{J/\psi} = (7.0 \pm 0.3) \times 10^{-6}$ is inferred. At 90% CL, the limits are $R_p < 2.8 \times 10^{-8}$ and $R_p^{J/\psi} < 6.5 \times 10^{-6}$.

In summary, a search for the $\bar{b}c$ annihilation process leading to B_c^+ meson decays into the $p\bar{p}\pi^+$ final state has been performed for the fiducial region $m(p\bar{p}) < 2.85 \text{ GeV}/c^2$, $p_T(B) < 20 \text{ GeV}/c$ and $2.0 < y(B) < 4.5$. No signal is observed and a 95% confidence level upper limit is inferred,

$$R_p = \frac{f_c}{f_u} \times \mathcal{B}(B_c^+ \rightarrow p\bar{p}\pi^+) < 3.6 \times 10^{-8}.$$

Acknowledgements

We express our gratitude to our colleagues in the CERN accelerator departments for the excellent performance of the LHC. We thank the technical and administrative staff at the LHCb institutes. We acknowledge support from CERN and from the na-

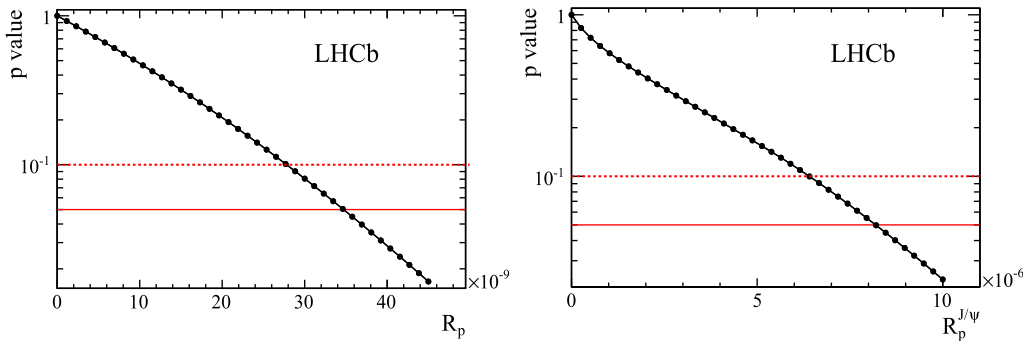


Fig. 5. p -value profile for (left) R_p and (right) $R_p^{J/\psi}$. The horizontal red solid and dashed lines indicate the 5% and 10% confidence levels. (For interpretation of the references to color in this figure legend, the reader is referred to the web version of this article.)

tional agencies: CAPES, CNPq, FAPERJ and FINEP (Brazil); NSFC (China); CNRS/IN2P3 (France); BMBF, DFG and MPG (Germany); INFN (Italy); FOM and NWO (The Netherlands); MNiSW and NCN (Poland); MEN/IFA (Romania); MinES and FANO (Russia); MINECO (Spain); SNSF and SER (Switzerland); NASU (Ukraine); STFC (United Kingdom); NSF (USA). We acknowledge the computing resources that are provided by CERN, IN2P3 (France), KIT and DESY (Germany), INFN (Italy), SURF (The Netherlands), PIC (Spain), GridPP (United Kingdom), RRCKI and Yandex LLC (Russia), CSCS (Switzerland), IFIN-HH (Romania), CBPF (Brazil), PL-GRID (Poland) and OSC (USA). We are indebted to the communities behind the multiple open source software packages on which we depend. Individual groups or members have received support from AvH Foundation (Germany), EPLANET, Marie Skłodowska-Curie Actions and ERC (European Union), Conseil Général de Haute-Savoie, Labex ENIGMASS and OCEVU, Région Auvergne (France), RFBR and Yandex LLC (Russia), GVA, XuntaGal and GENCAT (Spain), Herchel Smith Fund, The Royal Society, Royal Commission for the Exhibition of 1851 and the Leverhulme Trust (United Kingdom).

References

- [1] S. Descotes-Genon, et al., Non-leptonic charmless B_c decays and their search at LHCb, *Phys. Rev. D* 80 (2009) 114031, arXiv:0907.2256.
- [2] X. Liu, Z.-J. Xiao, C.-D. Lu, The pure annihilation type B_c to $M_2 M_3$ decays in the perturbative QCD approach, *Phys. Rev. D* 81 (2010) 014022, arXiv:0912.1163.
- [3] Z.-J. Xiao, X. Liu, The two-body hadronic decays of B_c meson in the perturbative QCD approach: a short review, *Chin. Sci. Bull.* 59 (2014) 3748, arXiv:1401.0151.
- [4] W.-S. Hou, Enhanced charged Higgs boson effects in $B^- \rightarrow \tau \bar{\nu}, \mu \bar{\nu}$ and $b \rightarrow \tau \bar{\nu} + X$, *Phys. Rev. D* 48 (1993) 2342.
- [5] S. Kanemura, M. Kikuchi, K. Yagyu, Fingerprinting the extended Higgs sector using one-loop corrected Higgs boson couplings and future precision measurements, *Nucl. Phys. B* 896 (2015) 80.
- [6] LHCb Collaboration, A.A. Alves Jr., et al., The LHCb detector at the LHC, *J. Instrum.* 3 (2008) S08005.
- [7] LHCb Collaboration, R. Aaij, et al., LHCb detector performance, *Int. J. Mod. Phys. A* 30 (2015) 1530022, arXiv:1412.6352.
- [8] R. Aaij, et al., The LHCb trigger and its performance in 2011, *J. Instrum.* 8 (2013) P04022, arXiv:1211.3055.
- [9] V.V. Gligorov, M. Williams, Efficient, reliable and fast high-level triggering using a bonsai boosted decision tree, *J. Instrum.* 8 (2013) P02013, arXiv:1210.6861.
- [10] T. Sjöstrand, S. Mrenna, P. Skands, A brief introduction to PYTHIA 8.1, *Comput. Phys. Commun.* 178 (2008) 852, arXiv:0710.3820.
- [11] C.-H. Chang, et al., BCVEPY: an event generator for hadronic production of the B_c meson, *Comput. Phys. Commun.* 159 (2004) 192, arXiv:hep-ph/0309120.
- [12] I. Belyaev, et al., Handling of the generation of primary events in Gauss, the LHCb simulation framework, *J. Phys. Conf. Ser.* 331 (2011) 032047.
- [13] D.J. Lange, The EvtGen particle decay simulation package, *Nucl. Instrum. Methods A* 462 (2001) 152.
- [14] P. Golonka, Z. Was, PHOTOS Monte Carlo: a precision tool for QED corrections in Z and W decays, *Eur. Phys. J. C* 45 (2006) 97, arXiv:hep-ph/0506026.
- [15] Geant4 Collaboration, J. Allison, et al., Geant4 developments and applications, *IEEE Trans. Nucl. Sci.* 53 (2006) 270;
- [16] Geant4 Collaboration, S. Agostinelli, et al., Geant4: a simulation toolkit, *Nucl. Instrum. Methods A* 506 (2003) 250.
- [17] M. Clemencic, et al., The LHCb simulation application, Gauss: design, evolution and experience, *J. Phys. Conf. Ser.* 331 (2011) 032023.
- [18] LHCb Collaboration, R. Aaij, et al., Measurement of B_c^+ production at $\sqrt{s} = 8$ TeV, *Phys. Rev. Lett.* 114 (2015) 132001, arXiv:1411.2943.
- [19] T. Skwarnicki, A study of the radiative cascade transitions between the Upsilon-prime and Upsilon resonances, PhD thesis, Institute of Nuclear Physics, Krakow, 1986, DESY-F31-86-02.
- [20] LHCb Collaboration, R. Aaij, et al., Evidence for CP violation in $B^+ \rightarrow p\bar{p}K^+$ decays, *Phys. Rev. Lett.* 113 (2014) 141801, arXiv:1407.5907.
- [21] M. Pivk, F.R. Le Diberder, sPlot: a statistical tool to unfold data distributions, *Nucl. Instrum. Methods A* 555 (2005) 356, arXiv:physics/0402083.
- [22] Heavy Flavor Averaging Group, Y. Amhis, et al., Averages of b -hadron, c -hadron, and τ -lepton properties as of summer 2014, arXiv:1412.7515, updated results and plots available at <http://www.slac.stanford.edu/xorg/hfag/>.
- [23] Particle Data Group, K.A. Olive, et al., Review of particle physics *Chin. Phys. C* 38 (2014) 090001, and 2015 update.
- [24] G. Cowan, et al., Asymptotic formulae for likelihood-based tests of new physics, *Eur. Phys. J. C* 71 (2011) 1554, arXiv:1007.1727.

LHCb Collaboration

R. Aaij ³⁹, C. Abellán Beteta ⁴¹, B. Adeva ³⁸, M. Adinolfi ⁴⁷, Z. Ajaltouni ⁵, S. Akar ⁶, J. Albrecht ¹⁰, F. Alessio ³⁹, M. Alexander ⁵², S. Ali ⁴², G. Alkhazov ³¹, P. Alvarez Cartelle ⁵⁴, A.A. Alves Jr ⁵⁸, S. Amato ², S. Amerio ²³, Y. Amhis ⁷, L. An ^{3,40}, L. Anderlini ¹⁸, G. Andreassi ⁴⁰, M. Andreotti ^{17,g}, J.E. Andrews ⁵⁹, R.B. Appleby ⁵⁵, O. Aquines Gutierrez ¹¹, F. Archilli ³⁹, P. d'Argent ¹², A. Artamonov ³⁶, M. Artuso ⁶⁰, E. Aslanides ⁶, G. Auriemma ^{26,n}, M. Baalouch ⁵, S. Bachmann ¹², J.J. Back ⁴⁹, A. Badalov ³⁷, C. Baesso ⁶¹, S. Baker ⁵⁴, W. Baldini ¹⁷, R.J. Barlow ⁵⁵, C. Barschel ³⁹, S. Barsuk ⁷, W. Barter ³⁹, V. Batozskaya ²⁹, V. Battista ⁴⁰, A. Bay ⁴⁰, L. Beaucourt ⁴, J. Beddow ⁵², F. Bedeschi ²⁴, I. Bediaga ¹, L.J. Bel ⁴², V. Bellee ⁴⁰, N. Belloli ^{21,k}, I. Belyaev ³², E. Ben-Haim ⁸, G. Bencivenni ¹⁹, S. Benson ³⁹, J. Benton ⁴⁷, A. Berezhnoy ³³, R. Bernet ⁴¹, A. Bertolin ²³, F. Betti ¹⁵, M.-O. Bettler ³⁹, M. van Beuzekom ⁴², S. Bifani ⁴⁶, P. Billoir ⁸, T. Bird ⁵⁵, A. Birnkraut ¹⁰, A. Bizzeti ^{18,i}, T. Blake ⁴⁹, F. Blanc ⁴⁰, J. Blouw ¹¹, S. Blusk ⁶⁰, V. Bocci ²⁶,

- A. Bondar ³⁵, N. Bondar ^{31,39}, W. Bonivento ¹⁶, A. Borgheresi ^{21,k}, S. Borghi ⁵⁵, M. Borisjak ⁶⁷,
 M. Borsato ³⁸, M. Boubdir ⁹, T.J.V. Bowcock ⁵³, E. Bowen ⁴¹, C. Bozzi ^{17,39}, S. Braun ¹², M. Britsch ¹²,
 T. Britton ⁶⁰, J. Brodzicka ⁵⁵, E. Buchanan ⁴⁷, C. Burr ⁵⁵, A. Bursche ², J. Buytaert ³⁹, S. Cadeddu ¹⁶,
 R. Calabrese ^{17,g}, M. Calvi ^{21,k}, M. Calvo Gomez ^{37,p}, P. Campana ¹⁹, D. Campora Perez ³⁹, L. Capriotti ⁵⁵,
 A. Carbone ^{15,e}, G. Carboni ^{25,l}, R. Cardinale ^{20,j}, A. Cardini ¹⁶, P. Carniti ^{21,k}, L. Carson ⁵¹,
 K. Carvalho Akiba ², G. Casse ⁵³, L. Cassina ^{21,k}, L. Castillo Garcia ⁴⁰, M. Cattaneo ³⁹, Ch. Cauet ¹⁰,
 G. Cavallero ²⁰, R. Cenci ^{24,t}, M. Charles ⁸, Ph. Charpentier ³⁹, G. Chatzikonstantinidis ⁴⁶, M. Chefdeville ⁴,
 S. Chen ⁵⁵, S.-F. Cheung ⁵⁶, M. Chrzaszcz ^{41,27}, X. Cid Vidal ³⁹, G. Ciezarek ⁴², P.E.L. Clarke ⁵¹,
 M. Clemencic ³⁹, H.V. Cliff ⁴⁸, J. Closier ³⁹, V. Coco ⁵⁸, J. Cogan ⁶, E. Cogneras ⁵, V. Cogoni ^{16,f},
 L. Cojocariu ³⁰, G. Collazuol ^{23,r}, P. Collins ³⁹, A. Comerma-Montells ¹², A. Contu ³⁹, A. Cook ⁴⁷,
 M. Coombes ⁴⁷, S. Coquereau ⁸, G. Corti ³⁹, M. Corvo ^{17,g}, B. Couturier ³⁹, G.A. Cowan ⁵¹, D.C. Craik ⁵¹,
 A. Crocombe ⁴⁹, M. Cruz Torres ⁶¹, S. Cunliffe ⁵⁴, R. Currie ⁵⁴, C. D'Ambrosio ³⁹, E. Dall'Occo ⁴²,
 J. Dalseno ⁴⁷, P.N.Y. David ⁴², A. Davis ⁵⁸, O. De Aguiar Francisco ², K. De Bruyn ⁶, S. De Capua ⁵⁵,
 M. De Cian ¹², J.M. De Miranda ¹, L. De Paula ², P. De Simone ¹⁹, C.-T. Dean ⁵², D. Decamp ⁴,
 M. Deckenhoff ¹⁰, L. Del Buono ⁸, N. Déléage ⁴, M. Demmer ¹⁰, D. Derkach ⁶⁷, O. Deschamps ⁵,
 F. Dettori ³⁹, B. Dey ²², A. Di Canto ³⁹, F. Di Ruscio ²⁵, H. Dijkstra ³⁹, F. Dordei ³⁹, M. Dorigo ⁴⁰,
 A. Dosil Suárez ³⁸, A. Dovbnya ⁴⁴, K. Dreimanis ⁵³, L. Dufour ⁴², G. Dujany ⁵⁵, K. Dungs ³⁹, P. Durante ³⁹,
 R. Dzhelyadin ³⁶, A. Dziurda ²⁷, A. Dzyuba ³¹, S. Easo ^{50,39}, U. Egede ⁵⁴, V. Egorychev ³², S. Eidelman ³⁵,
 S. Eisenhardt ⁵¹, U. Eitschberger ¹⁰, R. Ekelhof ¹⁰, L. Eklund ⁵², I. El Rifai ⁵, Ch. Elsasser ⁴¹, S. Ely ⁶⁰,
 S. Esen ¹², H.M. Evans ⁴⁸, T. Evans ⁵⁶, A. Falabella ¹⁵, C. Färber ³⁹, N. Farley ⁴⁶, S. Farry ⁵³, R. Fay ⁵³,
 D. Fazzini ^{21,k}, D. Ferguson ⁵¹, V. Fernandez Albor ³⁸, F. Ferrari ¹⁵, F. Ferreira Rodrigues ¹,
 M. Ferro-Luzzi ³⁹, S. Filippov ³⁴, M. Fiore ^{17,g}, M. Fiorini ^{17,g}, M. Firlej ²⁸, C. Fitzpatrick ⁴⁰, T. Fiutowski ²⁸,
 F. Fleuret ^{7,b}, K. Fohl ³⁹, M. Fontana ¹⁶, F. Fontanelli ^{20,j}, D.C. Forshaw ⁶⁰, R. Forty ³⁹, M. Frank ³⁹, C. Frei ³⁹,
 M. Frosini ¹⁸, J. Fu ²², E. Furfaro ^{25,l}, A. Gallas Torreira ³⁸, D. Galli ^{15,e}, S. Gallorini ²³, S. Gambetta ⁵¹,
 M. Gandelman ², P. Gandini ⁵⁶, Y. Gao ³, J. García Pardiñas ³⁸, J. Garra Tico ⁴⁸, L. Garrido ³⁷, P.J. Garsed ⁴⁸,
 D. Gascon ³⁷, C. Gaspar ³⁹, L. Gavardi ¹⁰, G. Gazzoni ⁵, D. Gerick ¹², E. Gersabeck ¹², M. Gersabeck ⁵⁵,
 T. Gershon ⁴⁹, Ph. Ghez ⁴, S. Gianì ⁴⁰, V. Gibson ⁴⁸, O.G. Girard ⁴⁰, L. Giubega ³⁰, V.V. Gligorov ³⁹,
 C. Göbel ⁶¹, D. Golubkov ³², A. Golutvin ^{54,39}, A. Gomes ^{1,a}, C. Gotti ^{21,k}, M. Grabalosa Gándara ⁵,
 R. Graciani Diaz ³⁷, L.A. Granado Cardoso ³⁹, E. Graugés ³⁷, E. Graverini ⁴¹, G. Graziani ¹⁸, A. Grecu ³⁰,
 P. Griffith ⁴⁶, L. Grillo ¹², O. Grünberg ⁶⁵, B. Gui ⁶⁰, E. Gushchin ³⁴, Yu. Guz ^{36,39}, T. Gys ³⁹,
 T. Hadavizadeh ⁵⁶, C. Hadjivasiliou ⁶⁰, G. Haefeli ⁴⁰, C. Haen ³⁹, S.C. Haines ⁴⁸, S. Hall ⁵⁴, B. Hamilton ⁵⁹,
 X. Han ¹², S. Hansmann-Menzemer ¹², N. Harnew ⁵⁶, S.T. Harnew ⁴⁷, J. Harrison ⁵⁵, J. He ³⁹, T. Head ⁴⁰,
 A. Heister ⁹, K. Hennessy ⁵³, P. Henrard ⁵, L. Henry ⁸, J.A. Hernando Morata ³⁸, E. van Herwijnen ³⁹,
 M. Heß ⁶⁵, A. Hicheur ^{2,*}, D. Hill ⁵⁶, M. Hoballah ⁵, C. Hombach ⁵⁵, L. Hongming ⁴⁰, W. Hulsbergen ⁴²,
 T. Humair ⁵⁴, M. Hushchyn ⁶⁷, N. Hussain ⁵⁶, D. Hutchcroft ⁵³, M. Idzik ²⁸, P. Ilten ⁵⁷, R. Jacobsson ³⁹,
 A. Jaeger ¹², J. Jalocha ⁵⁶, E. Jans ⁴², A. Jawahery ⁵⁹, M. John ⁵⁶, D. Johnson ³⁹, C.R. Jones ⁴⁸, C. Joram ³⁹,
 B. Jost ³⁹, N. Jurik ⁶⁰, S. Kandybei ⁴⁴, W. Kanso ⁶, M. Karacson ³⁹, T.M. Karbach ^{39,†}, S. Karodia ⁵²,
 M. Kecke ¹², M. Kelsey ⁶⁰, I.R. Kenyon ⁴⁶, M. Kenzie ³⁹, T. Ketel ⁴³, E. Khairullin ⁶⁷, B. Khanji ^{21,39,k},
 C. Khurewathanakul ⁴⁰, T. Kirn ⁹, S. Klaver ⁵⁵, K. Klimaszewski ²⁹, M. Kolpin ¹², I. Komarov ⁴⁰,
 R.F. Koopman ⁴³, P. Koppenburg ⁴², M. Kozeiha ⁵, L. Kravchuk ³⁴, K. Kreplin ¹², M. Kreps ⁴⁹, P. Krokovny ³⁵,
 F. Kruse ¹⁰, W. Krzemien ²⁹, W. Kucewicz ^{27,o}, M. Kucharczyk ²⁷, V. Kudryavtsev ³⁵, A.K. Kuonen ⁴⁰,
 K. Kurek ²⁹, T. Kvaratskheliya ³², D. Lacarrere ³⁹, G. Lafferty ^{55,39}, A. Lai ¹⁶, D. Lambert ⁵¹, G. Lanfranchi ¹⁹,
 C. Langenbruch ⁴⁹, B. Langhans ³⁹, T. Latham ⁴⁹, C. Lazzeroni ⁴⁶, R. Le Gac ⁶, J. van Leerdam ⁴², J.-P. Lees ⁴,
 R. Lefèvre ⁵, A. Leflat ^{33,39}, J. Lefrançois ⁷, E. Lemos Cid ³⁸, O. Leroy ⁶, T. Lesiak ²⁷, B. Leverington ¹², Y. Li ⁷,
 T. Likhomanenko ^{67,66}, R. Lindner ³⁹, C. Linn ³⁹, F. Lionetto ⁴¹, B. Liu ¹⁶, X. Liu ³, D. Loh ⁴⁹, I. Longstaff ⁵²,
 J.H. Lopes ², D. Lucchesi ^{23,r}, M. Lucio Martinez ³⁸, H. Luo ⁵¹, A. Lupato ²³, E. Luppi ^{17,g}, O. Lupton ⁵⁶,
 N. Lusardi ²², A. Lusiani ²⁴, X. Lyu ⁶², F. Machefert ⁷, F. Maciuc ³⁰, O. Maev ³¹, K. Maguire ⁵⁵, S. Malde ⁵⁶,
 A. Malinin ⁶⁶, G. Manca ⁷, G. Mancinelli ⁶, P. Manning ⁶⁰, A. Mapelli ³⁹, J. Maratas ⁵, J.F. Marchand ⁴,
 U. Marconi ¹⁵, C. Marin Benito ³⁷, P. Marino ^{24,t}, J. Marks ¹², G. Martellotti ²⁶, M. Martin ⁶, M. Martinelli ⁴⁰,
 D. Martinez Santos ³⁸, F. Martinez Vidal ⁶⁸, D. Martins Tostes ², L.M. Massacrier ⁷, A. Massafferri ¹,
 R. Matev ³⁹, A. Mathad ⁴⁹, Z. Mathe ³⁹, C. Matteuzzi ²¹, A. Mauri ⁴¹, B. Maurin ⁴⁰, A. Mazurov ⁴⁶,
 M. McCann ⁵⁴, J. McCarthy ⁴⁶, A. McNab ⁵⁵, R. McNulty ¹³, B. Meadows ⁵⁸, F. Meier ¹⁰, M. Meissner ¹²,

D. Melnychuk ²⁹, M. Merk ⁴², A. Merli ^{22,u}, E. Michielin ²³, D.A. Milanes ⁶⁴, M.-N. Minard ⁴, D.S. Mitzel ¹², J. Molina Rodriguez ⁶¹, I.A. Monroy ⁶⁴, S. Monteil ⁵, M. Morandin ²³, P. Morawski ²⁸, A. Mordà ⁶, M.J. Morello ^{24,t}, J. Moron ²⁸, A.B. Morris ⁵¹, R. Mountain ⁶⁰, F. Muheim ⁵¹, D. Müller ⁵⁵, J. Müller ¹⁰, K. Müller ⁴¹, V. Müller ¹⁰, M. Mussini ¹⁵, B. Muster ⁴⁰, P. Naik ⁴⁷, T. Nakada ⁴⁰, R. Nandakumar ⁵⁰, A. Nandi ⁵⁶, I. Nasteva ², M. Needham ⁵¹, N. Neri ²², S. Neubert ¹², N. Neufeld ³⁹, M. Neuner ¹², A.D. Nguyen ⁴⁰, C. Nguyen-Mau ^{40,q}, V. Niess ⁵, S. Nieswand ⁹, R. Niet ¹⁰, N. Nikitin ³³, T. Nikodem ¹², A. Novoselov ³⁶, D.P. O'Hanlon ⁴⁹, A. Oblakowska-Mucha ²⁸, V. Obraztsov ³⁶, S. Ogilvy ⁵², O. Okhrimenko ⁴⁵, R. Oldeman ^{16,48,f}, C.J.G. Onderwater ⁶⁹, B. Osorio Rodrigues ¹, J.M. Otalora Goicochea ², A. Otto ³⁹, P. Owen ⁵⁴, A. Oyanguren ⁶⁸, A. Palano ^{14,d}, F. Palombo ^{22,u}, M. Palutan ¹⁹, J. Panman ³⁹, A. Papanestis ⁵⁰, M. Pappagallo ⁵², L.L. Pappalardo ^{17,g}, C. Pappenheimer ⁵⁸, W. Parker ⁵⁹, C. Parkes ⁵⁵, G. Passaleva ¹⁸, G.D. Patel ⁵³, M. Patel ⁵⁴, C. Patrignani ^{20,j}, A. Pearce ^{55,50}, A. Pellegrino ⁴², G. Penso ^{26,m}, M. Pepe Altarelli ³⁹, S. Perazzini ^{15,e}, P. Perret ⁵, L. Pescatore ⁴⁶, K. Petridis ⁴⁷, A. Petrolini ^{20,j}, M. Petruzzo ²², E. Picatoste Olloqui ³⁷, B. Pietrzyk ⁴, M. Pikies ²⁷, D. Pinci ²⁶, A. Pistone ²⁰, A. Piucci ¹², S. Playfer ⁵¹, M. Plo Casasus ³⁸, T. Poikela ³⁹, F. Polci ⁸, A. Poluektov ^{49,35}, I. Polyakov ³², E. Polycarpo ², A. Popov ³⁶, D. Popov ^{11,39}, B. Popovici ³⁰, C. Potterat ², E. Price ⁴⁷, J.D. Price ⁵³, J. Prisciandaro ³⁸, A. Pritchard ⁵³, C. Prouve ⁴⁷, V. Pugatch ⁴⁵, A. Puig Navarro ⁴⁰, G. Punzi ^{24,s}, W. Qian ⁵⁶, R. Quagliani ^{7,47}, B. Rachwal ²⁷, J.H. Rademacker ⁴⁷, M. Rama ²⁴, M. Ramos Pernas ³⁸, M.S. Rangel ², I. Raniuk ⁴⁴, G. Raven ⁴³, F. Redi ⁵⁴, S. Reichert ⁵⁵, A.C. dos Reis ¹, V. Renaudin ⁷, S. Ricciardi ⁵⁰, S. Richards ⁴⁷, M. Rihl ³⁹, K. Rinnert ^{53,39}, V. Rives Molina ³⁷, P. Robbe ⁷, A.B. Rodrigues ¹, E. Rodrigues ⁵⁵, J.A. Rodriguez Lopez ⁶⁴, P. Rodriguez Perez ⁵⁵, A. Rogozhnikov ⁶⁷, S. Roiser ³⁹, V. Romanovsky ³⁶, A. Romero Vidal ³⁸, J.W. Ronayne ¹³, M. Rotondo ²³, T. Ruf ³⁹, P. Ruiz Valls ⁶⁸, J.J. Saborido Silva ³⁸, N. Sagidova ³¹, B. Saitta ^{16,f}, V. Salustino Guimaraes ², C. Sanchez Mayordomo ⁶⁸, B. Sanmartin Sedes ³⁸, R. Santacesaria ²⁶, C. Santamarina Rios ³⁸, M. Santimaria ¹⁹, E. Santovetti ^{25,l}, A. Sarti ^{19,m}, C. Satriano ^{26,n}, A. Satta ²⁵, D.M. Saunders ⁴⁷, D. Savrina ^{32,33}, S. Schael ⁹, M. Schiller ³⁹, H. Schindler ³⁹, M. Schlupp ¹⁰, M. Schmelling ¹¹, T. Schmelzer ¹⁰, B. Schmidt ³⁹, O. Schneider ⁴⁰, A. Schopper ³⁹, M. Schubiger ⁴⁰, M.-H. Schune ⁷, R. Schwemmer ³⁹, B. Sciascia ¹⁹, A. Sciubba ^{26,m}, A. Semennikov ³², A. Sergi ⁴⁶, N. Serra ⁴¹, J. Serrano ⁶, L. Sestini ²³, P. Seyfert ²¹, M. Shapkin ³⁶, I. Shapoval ^{17,44,g}, Y. Shcheglov ³¹, T. Shears ⁵³, L. Shekhtman ³⁵, V. Shevchenko ⁶⁶, A. Shires ¹⁰, B.G. Siddi ¹⁷, R. Silva Coutinho ⁴¹, L. Silva de Oliveira ², G. Simi ^{23,s}, M. Sirendi ⁴⁸, N. Skidmore ⁴⁷, T. Skwarnicki ⁶⁰, E. Smith ⁵⁴, I.T. Smith ⁵¹, J. Smith ⁴⁸, M. Smith ⁵⁵, H. Snoek ⁴², M.D. Sokoloff ⁵⁸, F.J.P. Soler ⁵², F. Soomro ⁴⁰, D. Souza ⁴⁷, B. Souza De Paula ², B. Spaan ¹⁰, P. Spradlin ⁵², S. Sridharan ³⁹, F. Stagni ³⁹, M. Stahl ¹², S. Stahl ³⁹, S. Stefkova ⁵⁴, O. Steinkamp ⁴¹, O. Stenyakin ³⁶, S. Stevenson ⁵⁶, S. Stoica ³⁰, S. Stone ⁶⁰, B. Storaci ⁴¹, S. Stracka ^{24,t}, M. Straticiuc ³⁰, U. Straumann ⁴¹, L. Sun ⁵⁸, W. Sutcliffe ⁵⁴, K. Swientek ²⁸, S. Swientek ¹⁰, V. Syropoulos ⁴³, M. Szczekowski ²⁹, T. Szumlak ²⁸, S. T'Jampens ⁴, A. Tayduganov ⁶, T. Tekampe ¹⁰, G. Tellarini ^{17,g}, F. Teubert ³⁹, C. Thomas ⁵⁶, E. Thomas ³⁹, J. van Tilburg ⁴², V. Tisserand ⁴, M. Tobin ⁴⁰, S. Tolk ⁴³, L. Tomassetti ^{17,g}, D. Tonelli ³⁹, S. Topp-Joergensen ⁵⁶, E. Tournefier ⁴, S. Tourneur ⁴⁰, K. Trabelsi ⁴⁰, M. Traill ⁵², M.T. Tran ⁴⁰, M. Tresch ⁴¹, A. Trisovic ³⁹, A. Tsaregorodtsev ⁶, P. Tsopelas ⁴², N. Tuning ^{42,39}, A. Ukleja ²⁹, A. Ustyuzhanin ^{67,66}, U. Uwer ¹², C. Vacca ^{16,39,f}, V. Vagnoni ^{15,39}, S. Valat ³⁹, G. Valenti ¹⁵, A. Vallier ⁷, R. Vazquez Gomez ¹⁹, P. Vazquez Regueiro ³⁸, C. Vázquez Sierra ³⁸, S. Vecchi ¹⁷, M. van Veghel ⁴², J.J. Velthuis ⁴⁷, M. Veltri ^{18,h}, G. Veneziano ⁴⁰, M. Vesterinen ¹², B. Viaud ⁷, D. Vieira ², M. Vieites Diaz ³⁸, X. Vilasis-Cardona ^{37,p}, V. Volkov ³³, A. Vollhardt ⁴¹, D. Voong ⁴⁷, A. Vorobyev ³¹, V. Vorobyev ³⁵, C. Voß ⁶⁵, J.A. de Vries ⁴², R. Waldi ⁶⁵, C. Wallace ⁴⁹, R. Wallace ¹³, J. Walsh ²⁴, J. Wang ⁶⁰, D.R. Ward ⁴⁸, N.K. Watson ⁴⁶, D. Websdale ⁵⁴, A. Weiden ⁴¹, M. Whitehead ³⁹, J. Wicht ⁴⁹, G. Wilkinson ^{56,39}, M. Wilkinson ⁶⁰, M. Williams ³⁹, M.P. Williams ⁴⁶, M. Williams ⁵⁷, T. Williams ⁴⁶, F.F. Wilson ⁵⁰, J. Wimberley ⁵⁹, J. Wishahi ¹⁰, W. Wislicki ²⁹, M. Witek ²⁷, G. Wormser ⁷, S.A. Wotton ⁴⁸, K. Wright ⁵², S. Wright ⁴⁸, K. Wyllie ³⁹, Y. Xie ⁶³, Z. Xu ⁴⁰, Z. Yang ³, H. Yin ⁶³, J. Yu ⁶³, X. Yuan ³⁵, O. Yushchenko ³⁶, M. Zangoli ¹⁵, M. Zavertyaev ^{11,c}, L. Zhang ³, Y. Zhang ³, A. Zhelezov ¹², Y. Zheng ⁶², A. Zhokhov ³², L. Zhong ³, V. Zhukov ⁹, S. Zucchelli ¹⁵

¹ Centro Brasileiro de Pesquisas Físicas (CBPF), Rio de Janeiro, Brazil² Universidade Federal do Rio de Janeiro (UFRJ), Rio de Janeiro, Brazil³ Center for High Energy Physics, Tsinghua University, Beijing, China⁴ LAPP, Université Savoie Mont-Blanc, CNRS/IN2P3, Annecy-Le-Vieux, France⁵ Clermont Université, Université Blaise Pascal, CNRS/IN2P3, LPC, Clermont-Ferrand, France⁶ CPPM, Aix-Marseille Université, CNRS/IN2P3, Marseille, France

- ⁷ LAL, Université Paris-Sud, CNRS/IN2P3, Orsay, France
⁸ LPNHE, Université Pierre et Marie Curie, Université Paris Diderot, CNRS/IN2P3, Paris, France
⁹ I. Physikalisches Institut, RWTH Aachen University, Aachen, Germany
¹⁰ Fakultät Physik, Technische Universität Dortmund, Dortmund, Germany
¹¹ Max-Planck-Institut für Kernphysik (MPIK), Heidelberg, Germany
¹² Physikalisches Institut, Ruprecht-Karls-Universität Heidelberg, Heidelberg, Germany
¹³ School of Physics, University College Dublin, Dublin, Ireland
¹⁴ Sezione INFN di Bari, Bari, Italy
¹⁵ Sezione INFN di Bologna, Bologna, Italy
¹⁶ Sezione INFN di Cagliari, Cagliari, Italy
¹⁷ Sezione INFN di Ferrara, Ferrara, Italy
¹⁸ Sezione INFN di Firenze, Firenze, Italy
¹⁹ Laboratori Nazionali dell'INFN di Frascati, Frascati, Italy
²⁰ Sezione INFN di Genova, Genova, Italy
²¹ Sezione INFN di Milano Bicocca, Milano, Italy
²² Sezione INFN di Milano, Milano, Italy
²³ Sezione INFN di Padova, Padova, Italy
²⁴ Sezione INFN di Pisa, Pisa, Italy
²⁵ Sezione INFN di Roma Tor Vergata, Roma, Italy
²⁶ Sezione INFN di Roma La Sapienza, Roma, Italy
²⁷ Henryk Niewodniczanski Institute of Nuclear Physics Polish Academy of Sciences, Kraków, Poland
²⁸ AGH – University of Science and Technology, Faculty of Physics and Applied Computer Science, Kraków, Poland
²⁹ National Center for Nuclear Research (NCBJ), Warsaw, Poland
³⁰ Horia Hulubei National Institute of Physics and Nuclear Engineering, Bucharest-Magurele, Romania
³¹ Petersburg Nuclear Physics Institute (PNPI), Gatchina, Russia
³² Institute of Theoretical and Experimental Physics (ITEP), Moscow, Russia
³³ Institute of Nuclear Physics, Moscow State University (SINP MSU), Moscow, Russia
³⁴ Institute for Nuclear Research of the Russian Academy of Sciences (INR RAN), Moscow, Russia
³⁵ Budker Institute of Nuclear Physics (SB RAS) and Novosibirsk State University, Novosibirsk, Russia
³⁶ Institute for High Energy Physics (IHEP), Protvino, Russia
³⁷ Universitat de Barcelona, Barcelona, Spain
³⁸ Universidad de Santiago de Compostela, Santiago de Compostela, Spain
³⁹ European Organization for Nuclear Research (CERN), Geneva, Switzerland
⁴⁰ Ecole Polytechnique Fédérale de Lausanne (EPFL), Lausanne, Switzerland
⁴¹ Physik-Institut, Universität Zürich, Zürich, Switzerland
⁴² Nikhef National Institute for Subatomic Physics, Amsterdam, The Netherlands
⁴³ Nikhef National Institute for Subatomic Physics and VU University Amsterdam, Amsterdam, The Netherlands
⁴⁴ NSC Kharkiv Institute of Physics and Technology (NSC KIPT), Kharkiv, Ukraine
⁴⁵ Institute for Nuclear Research of the National Academy of Sciences (KINR), Kyiv, Ukraine
⁴⁶ University of Birmingham, Birmingham, United Kingdom
⁴⁷ H.H. Wills Physics Laboratory, University of Bristol, Bristol, United Kingdom
⁴⁸ Cavendish Laboratory, University of Cambridge, Cambridge, United Kingdom
⁴⁹ Department of Physics, University of Warwick, Coventry, United Kingdom
⁵⁰ STFC Rutherford Appleton Laboratory, Didcot, United Kingdom
⁵¹ School of Physics and Astronomy, University of Edinburgh, Edinburgh, United Kingdom
⁵² School of Physics and Astronomy, University of Glasgow, Glasgow, United Kingdom
⁵³ Oliver Lodge Laboratory, University of Liverpool, Liverpool, United Kingdom
⁵⁴ Imperial College London, London, United Kingdom
⁵⁵ School of Physics and Astronomy, University of Manchester, Manchester, United Kingdom
⁵⁶ Department of Physics, University of Oxford, Oxford, United Kingdom
⁵⁷ Massachusetts Institute of Technology, Cambridge, MA, United States
⁵⁸ University of Cincinnati, Cincinnati, OH, United States
⁵⁹ University of Maryland, College Park, MD, United States
⁶⁰ Syracuse University, Syracuse, NY, United States
⁶¹ Pontifícia Universidade Católica do Rio de Janeiro (PUC-Rio), Rio de Janeiro, Brazil ^v
⁶² University of Chinese Academy of Sciences, Beijing, China ^w
⁶³ Institute of Particle Physics, Central China Normal University, Wuhan, Hubei, China ^w
⁶⁴ Departamento de Física, Universidad Nacional de Colombia, Bogota, Colombia ^x
⁶⁵ Institut für Physik, Universität Rostock, Rostock, Germany ^y
⁶⁶ National Research Centre Kurchatov Institute, Moscow, Russia ^z
⁶⁷ Yandex School of Data Analysis, Moscow, Russia ^z
⁶⁸ Instituto de Física Corpuscular (IFIC), Universitat de València-CSIC, Valencia, Spain ^{aa}
⁶⁹ Van Swinderen Institute, University of Groningen, Groningen, The Netherlands ^{ab}

* Corresponding author.

E-mail address: hicheur@if.ufrj.br (A. Hicheur).

^a Universidade Federal do Triângulo Mineiro (UFTM), Uberaba-MG, Brazil.

^b Laboratoire Leprince-Ringuet, Palaiseau, France.

^c P.N. Lebedev Physical Institute, Russian Academy of Science (LPI RAS), Moscow, Russia.

^d Università di Bari, Bari, Italy.

^e Università di Bologna, Bologna, Italy.

^f Università di Cagliari, Cagliari, Italy.

^g Università di Ferrara, Ferrara, Italy.

^h Università di Urbino, Urbino, Italy.

ⁱ Università di Modena e Reggio Emilia, Modena, Italy.

^j Università di Genova, Genova, Italy.

^k Università di Milano Bicocca, Milano, Italy.

- ^l Università di Roma Tor Vergata, Roma, Italy.
^m Università di Roma La Sapienza, Roma, Italy.
ⁿ Università della Basilicata, Potenza, Italy.
^o AGH – University of Science and Technology, Faculty of Computer Science, Electronics and Telecommunications, Kraków, Poland.
^p LIFAELS, La Salle, Universitat Ramon Llull, Barcelona, Spain.
^q Hanoi University of Science, Hanoi, Viet Nam.
^r Università di Padova, Padova, Italy.
^s Università di Pisa, Pisa, Italy.
^t Scuola Normale Superiore, Pisa, Italy.
^u Università degli Studi di Milano, Milano, Italy.
^v Associated to Universidade Federal do Rio de Janeiro (UFRJ), Rio de Janeiro, Brazil.
^w Associated to Center for High Energy Physics, Tsinghua University, Beijing, China.
^x Associated to LPNHE, Université Pierre et Marie Curie, Université Paris Diderot, CNRS/IN2P3, Paris, France.
^y Associated to Physikalisches Institut, Ruprecht-Karls-Universität Heidelberg, Heidelberg, Germany.
^z Associated to Institute of Theoretical and Experimental Physics (ITEP), Moscow, Russia.
^{aa} Associated to Universitat de Barcelona, Barcelona, Spain.
^{ab} Associated to Nikhef National Institute for Subatomic Physics, Amsterdam, The Netherlands.
† Deceased.